ELSEVIER

Polymer Vol. 37 No. 8, pp. 1317–1322, 1996

0032-3861/96/$15.00+0.00

Gaussian chains with excluded volume and hydrodynamic interaction: shear rate dependence of radius of gyration, intrinsic viscosity and flow birefringence

K. D. Knudsen* and J. García de la Torre
Departamento de Química Física, Facultad de Química, Universidad de Murcia, 30071 Murcia, Spain

and A. Elgsaeter
Department of Physics, Faculty of Physics and Mathematics, University of Trondheim, 7034 Trondheim, Norway
(Received 4 January 1995)

The effect of excluded volume (EV) and hydrodynamic interaction (HI) on a dilute solution of flexible polymer chains situated in a shear field has been studied by means of a Brownian dynamics simulation. The polymer was modelled as a Gaussian chain, accounting for the excluded volume effect by means of an exponentially decaying repulsive potential. The hydrodynamic interaction was included by means of the Rotne–Prager–Yamakawa tensor. The parameters studied were the mean square radius of gyration, the intrinsic viscosity, and the differential polarizability and extinction angle that are parameters relevant in flow birefringence studies. The EV-effect is seen to be most important at low shear rate. This is followed by an intermediate region where EV falls off and HI still has considerable effect, ending up with a chain that is so stretched out that neither EV nor HI has influence on conformational or hydrodynamical properties, giving parameter values in accordance with theory for the no-EV, no-HI case. Copyright © 1996 Elsevier Science Ltd.

INTRODUCTION

The excluded volume effect, that is the increase in chain dimensions due to short-range repulsion between different parts of a flexible chain, has been studied mainly at equilibrium conditions or in weak flows. Theoretical work[1] and computer simulations[2–4] have given information about the expansion of Gaussian chains in a situation where flow is not present. However, if a solution of flexible chains is situated for instance in a shear field, the chain will expand due to the friction forces between the chain segments and the surrounding solution, and this will in turn influence the excluded volume forces, since these depend on the distances between the different parts of the chain.

When a Gaussian chain is introduced into a shear field, the chain will experience an expansion which is theoretically given by the expression[5]: $\langle S^2\rangle = \langle S_0^2\rangle[1 + (16/945)N^4\lambda_H^2 g^2]$, where λ_H is a constant and g is the shear rate. $\langle S_0^2\rangle$ is the equilibrium square radius of gyration. In this formula neither hydrodynamic interaction nor excluded volume have been taken into account. The increase in $\langle S^2\rangle$ is caused by the flow field only. Thus, according to this equation, when hydrodynamic interaction and excluded volume are disregarded, the square radius of gyration will depend on the shear rate to the second power, and on the number of beads in the chain (N) to the fourth power. López Cascales *et al.*[6] have made a study on the shear rate dependence of $\langle S^2\rangle$, considering also the case with hydrodynamic interaction. However, to our knowledge no studies have been made upon the relation between $\langle S^2\rangle$ and N or g when both hydrodynamic interaction and excluded volume are taken into account.

We wanted in this work to make a qualitative study of the influence of the excluded volume effect on the behaviour of a dilute solution of flexible polymer chains in shear flow, examining, apart from the radius of gyration, the intrinsic viscosity and flow birefringence parameters.

THEORY AND MODELS

Polymer model

The polymer chain was modelled as a Gaussian bead-spring chain in which the behaviour of the springs is Hookean with potential energy $V = Hq^2/2$. The spring constant H equals $3kT/b^2$ and q is the instantaneous spring length. The parameter b is the root mean square spring length. A chain consists of N beads and $(N-1)$ springs. Each bead will experience a friction with respect

* To whom correspondence should be addressed

to the surrounding medium reflected by the friction coefficient $\zeta = 6\pi\eta_s\sigma$, where η_s is the solvent viscosity and σ is the hydrodynamic radius of the bead, taken to be[2] $\sigma = 0.256b$. In the simulations N has been equal to 20, apart from in the scaling law studies, where N has taken values from 6 to 37.

Excluded volume

To the model outlined above we have added repulsive interactions between non-neighboring units as a way to introduce the excluded volume effect. The interaction potential has the form

$$V_c(R_{ij}) = \begin{cases} Ae^{-\alpha R_{ij}}, & R_{ij} \leqslant r_c \\ 0, & R_{ij} > r_c \end{cases} \quad (1)$$

where R_{ij} is the interbead distance, A is a constant for the potential strength, α is a parameter defining the potential sharpness, and r_c is a cut-off distance for the excluded volume interaction.

With a proper value for α, this is a relatively soft potential, similar to the repulsive component of some typical intermolecular potentials for small molecules. This potential has the advantage that the time step in the Brownian dynamics simulations can be maintained at the same value as without the excluded volume effect. When sharper potentials are used, such as the Lennard–Jones, it may be necessary to reduce the time step by a factor of 100 to get correct results, with a corresponding unpleasant increase in computer time. The applicability of this soft potential has been tested in equilibrium conditions by Rey *et al.*[3], and they established values for the parameters A, α and r_c in equation (1) as: $A = 75.0$, $\alpha = 4$ and $r_c = 0.512$ (in dimensionless form, see below), which are the parameter values that we will use in our study.

In the simulations, the hydrodynamic interaction between beads in the chain has been included by means of the Rotne–Prager–Yamakawa tensor[7].

Simulation method

Trajectories in space for the bead-spring chains were obtained by means of the Brownian dynamics simulation technique and averages over the trajectory (after steady state had been reached) were used to calculate values for the parameters of interest ($\langle S^2\rangle$, $\langle R^2\rangle$, etc.). The BD-algorithm used was that of Ermak and McCammon[8], including a second-order modification by Iniesta and García de la Torre[9]. In the simulations dimensionless parameters were used. Lengths were divided by b, forces by kT/b, and time by $\zeta b^2/kT$. Other dimensionless quantities follow from these definitions. The relation between the shear rate, denoted g, and its dimensionless version, g^*, is in this scheme: $g^* = (6\pi\eta_s\sigma b^2/kT)g$, and the dimensionless form of the parameters $\langle S^2\rangle$ and $\langle R^2\rangle$ were denoted $\langle S^2\rangle^*$ and $\langle R^2\rangle^*$, respectively. The trajectory of each molecule was simulated starting from a generated random conformation, and the time step (in dimensionless units) was $\Delta t^* = 0.01$. Each trajectory consisted of 1×10^6 steps, and the first 10^5 steps were usually rejected because this represents a transition period before steady-state is reached. More detailed information on the simulation procedure can be found in the article by López Cascales and García de la Torre[10].

Intrinsic viscosity

The viscosity in simple shear $v_x = gy$, $v_y = v_z = 0$, is given by $\eta = \tau_{xy}/g$, where τ_{xy} is the stress. If we then use the expression for the strain tensor given by Bird *et al.*[11], we obtain a formula for calculating the intrinsic viscosity at shear rate g

$$[\eta] = \sum_j \frac{N_A\langle Q_{jx}F_{jy}\rangle}{\eta_s g M} \quad (2)$$

where N_A is Avogadro's number, Q_{jx} is the projection onto the x-axis of the connector between bead j and $j+1$, F_{jy} is the spring force in direction y on bead j, and M is the molecular weight. The dimensionless form of this equation (used in the simulations) is

$$[\eta]^* = \frac{6\pi\sigma}{g^*}\sum\langle Q_{jx}^* F_{jy}^*\rangle \quad (3)$$

Flow birefringence

When a polymer solution is subjected to flow, birefringence may result due to the orientation of chain segments that have different polarizability along and perpendicular to the segment. Flow birefringence is a sensitive experimental tool for measuring conformational properties, and the two parameters of interest are the differential polarizability, $\Delta\Gamma$, and the extinction angle, χ. The differential polarizability (along the principal axes of the polarizability tensor) is given by[12]

$$\Delta\Gamma = 3C[(\langle \mathbf{x}^t\mathbf{A}\mathbf{x}\rangle - \langle \mathbf{y}^T\mathbf{A}\mathbf{y}\rangle)^2 + 4\langle \mathbf{x}^T\mathbf{A}\mathbf{y}\rangle^2]^{1/2} \quad (4)$$

where C is a system constant, $\mathbf{x}$, $\mathbf{y}$ the N-dimensional vectors containing the coordinates of the beads in the chain and $\mathbf{A}$ is a transformation matrix. The extinction angle can be found from[12]

$$\tan 2\chi = \frac{2\langle \mathbf{x}^T\mathbf{A}\mathbf{y}\rangle}{\langle \mathbf{x}^T\mathbf{A}\mathbf{x}\rangle - \langle \mathbf{y}^T\mathbf{A}\mathbf{y}\rangle} \quad (5)$$

If we instead of $\Delta\Gamma$ make use of its reduced version $\Delta\Gamma = \Delta\Gamma/3Cb^2$, the two expressions above are suitable for calculating these two parameters in a computer simulation, and we will use them to look at the influence of EV on flow birefringence.

RESULTS AND DISCUSSION

According to theory[11], the square radius of gyration for a Gaussian chain without excluded volume at equilibrium is: $\langle S_0^2\rangle = b^2(N^2-1)/6N$. A log–log plot of $\langle S_0^2\rangle$ vs $(N^2-1)/N$ will thus have an exponent equal to 1. The same is the case when $\langle R^2\rangle$ is plotted *versus* $(N-1)$, since the equilibrium expression for this parameter is $\langle R^2\rangle = (N-1)b^2$. However, when excluded volume is introduced, the chain will expand, and according to Renormalization Group Theory[1] the exponent (named 2ν) will take the value 1.176. As a test of the simulation routine and the applied excluded volume potential, we started our simulations with a study of Gaussian chains at equilibrium, to check the exponents obtained against the value mentioned above.

Figures 1a and *b* show the results of simulations with Gaussian chains at equilibrium, i.e. no shear field, and with excluded volume and hydrodynamic interaction

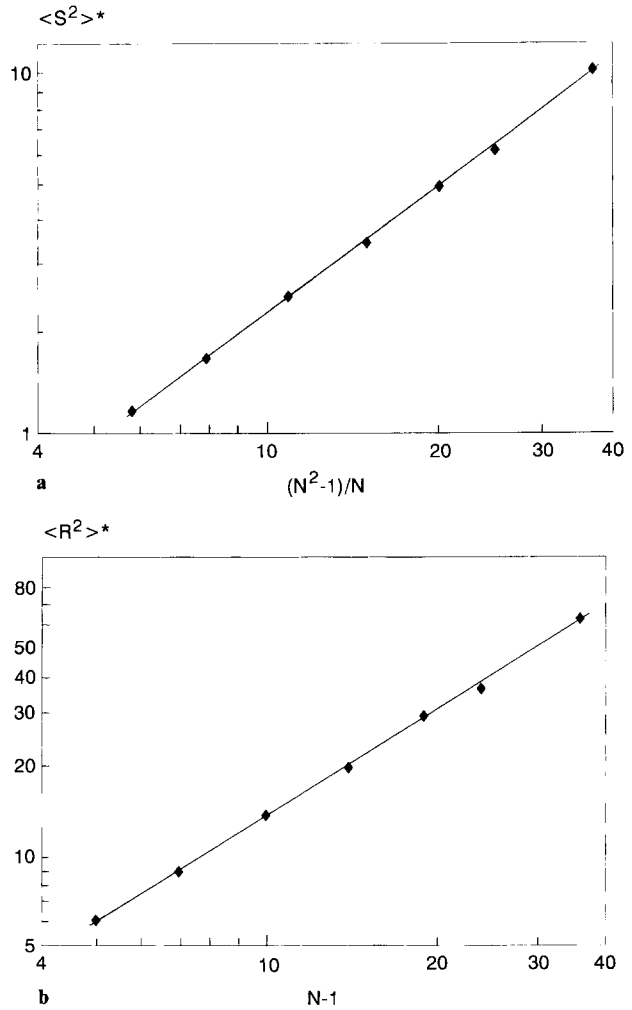

Figure 1 (a) Mean square radius of gyration (in dimensionless form) *versus* $(N^2 - 1)/N$ (where N is number of beads) for Gaussian chains at equilibrium (log–log plot). The effects of excluded volume (EV) and hydrodynamic interaction (HI) were included in the simulation. (b) Mean square end–end distance (in dimensionless form) *versus* $(N - 1)$ for Gaussian chains at equilibrium (log–log plot). The effects of excluded volume (EV) and hydrodynamic interaction (HI) were included in the simulation

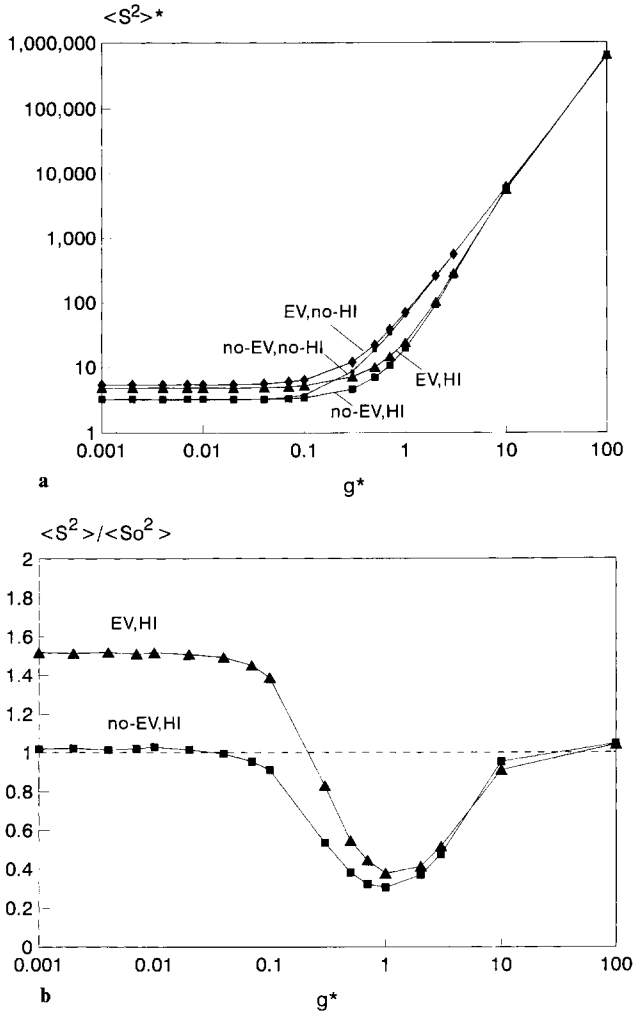

Figure 2 (a) Mean square radius of gyration (in dimensionless form) *versus* dimensionless shear rate for a 20-bead Gaussian chain. Four cases are shown: without excluded volume (EV) and without hydrodynamic interaction (no-EV, no-HI); with EV and without HI (EV, no-HI); without EV and with HI (no-EV, HI); with EV and with HI (EV, HI). (b) Relative mean square radius of gyration *versus* dimensionless shear rate for a 20-bead Gaussian chain. The curves marked EV, HI and no-EV, HI are the simulation results for these cases divided by results from the no-EV, no-HI case

effects included. The values of the dimensionless mean square radius of gyration, $\langle S^2 \rangle^*$, and the dimensionless mean square end–end distance, $\langle R^2 \rangle^*$, are plotted *versus* $(N^2 - 1)/N$ and $N - 1$, respectively. In this simulation we have used a range of different N-values (from 6 to 37 beads in the chain). As explained above, theoretical predictions for the scaling relationship between $\langle S^2 \rangle^*$ and $(N^2 - 1)/N$ and between $\langle R^2 \rangle^*$ and $N - 1$ give an exponent equal to 1.176. From our simulations we obtain the exponents 1.173 ± 0.008 and 1.172 ± 0.008, respectively, a result that is taken as a confirmation of the validity of the applied excluded volume potential and the simulation algorithm.

In *Figure 2a* is shown in a log–log plot our simulation results for $\langle S^2 \rangle^*$ for a 20-bead Gaussian chain *versus* dimensionless shear rate. For comparison, apart from the EV-HI case, the results for the cases without hydrodynamic interaction (no-HI) and without excluded volume (no-EV) are also shown in this figure. It is seen how the behaviour as a function of the shear rate can be divided into two separate regimes, one at low shear rates (g^* up to approx. 0.1) where $\langle S^2 \rangle^*$ is nearly constant, and one at higher shear rates, where the value of $\langle S^{2*} \rangle$ increases drastically with the shear rate. Since in *Figure 2a* the no-HI and HI curves at low shear rates lie much closer than the no-EV and EV curves, it is seen that the EV effect is more important than the HI effect in this regime. In the transition region from $g^* = 0.1$ to around 1.0, the EV effect is seen to disappear (no distinction between no-EV and EV curves), and only the effect of HI remains. This is reasonable since the effect of EV is important only when the beads are situated very close to each other, thus reducing its importance at high shear. The influence of HI finally disappears around $g^* = 10$. Above this shear rate, the mean square radius of gyration is found to vary with the second power of the shear rate, in accordance with theoretical predictions[13] and earlier simulation results[14]. The large extension that is seen for high values of the shear rate is unrealistic for a real polymer chain since this will have a finite limit to the extension governed by its contour length, and will break

if the force on the polymer is sufficiently high. However, the simulation results for high shear are interesting for comparison with theory and for illustration of the shear rate dependence of the EV and HI effects.

In *Figure 2b* is seen how the relationship $\langle S^2\rangle/\langle S_0^2\rangle$ (where $\langle S_0^2\rangle$ refers to the no-EV, no-HI case) varies with the shear rate for the cases with and without EV. In the EV-HI case, from a starting value above 1, $\langle S^2\rangle/\langle S_0^2\rangle$ passes through a minimum and finally reaches the value 1, corresponding to the case of negligible influence of EV and HI. The expansion of the chain at low shear due to EV, represented by the value $\langle S^2\rangle$, is found to be approximately 50%. The drop in the ratio $\langle S^2\rangle/\langle S_0^2\rangle$ at intermediate shear rates, i.e. the observed relative compression of the molecule, is due to the following. At low shear rates, when the chain molecule has a rather compact form, the EV effect dominates and the molecule is expanded compared to the situation where this effect is not taken into account (phantom chain). However, when the shear rate is increased, the EV effect starts to diminish and the influence of HI starts to be comparable with EV. Since the effect of HI on the polymer chain always is that of a reduction in chain dimensions, a fact that also can be seen in *Figure 2a*, the ratio $\langle S^2\rangle/\langle S_0^2\rangle$ will start to fall. It will reach a minimum when the EV effect has almost disappeared, but the HI effect still is significant. From *Figure 2b* this is found to take place around $g^* = 1$, with a minimum of approximately 0.4.

Figure 3 shows our simulation results for the dimensionless intrinsic viscosity of the polymer chains *versus* dimensionless shear rate in a log–log plot. Three cases are shown; (a) only HI included, (b) only EV included, and (c) both EV and HI included. We can see that the inclusion of one or both of these effects results in a shear-dependent intrinsic viscosity, an observation made also in other works[10,15]. If only HI (and not EV) is taken into account, a significant shear-thickening behaviour is observed, whereas if only EV is considered, we see a clear shear-thinning behaviour. The latter result is explained by the fact that the intrinsic viscosity is directly related to the chain dimensions, which contribution from EV diminishes as the EV-effect is reduced with increasing shear rate. The shear-thickening behaviour found with HI is explained by the fact that since HI reduces the chain dimensions, this will lower the value of the intrinsic viscosity, but this effect will disappear as HI is reduced with increasing shear rate. At high shear rates the curves converge to the no-EV, no-HI value, similar to what was found for $\langle S^2\rangle^*$. When both EV and HI are included, a situation that should be closer to that of a real system, we obtain a small lowering in the intrinsic viscosity at the start, followed by a shear-thickening region. The first part is similar to what is observed experimentally for flexible chains, whereas the final increase in viscosity is a non-real feature, a result that illustrates the well known fact that the Gaussian model is not realistic at very high shear rates.

In *Figures 4a* and *b* are shown our simulation results for the value of the birefringence of the sample of polymer chains *versus* dimensionless shear rate in log–log plots. *Figure 4a* shows the effect of EV on the differential polarizability $\Delta\Gamma'$. The influence of excluded volume is greatest for small values of the shear rate, as mentioned in connection with the parameters discussed

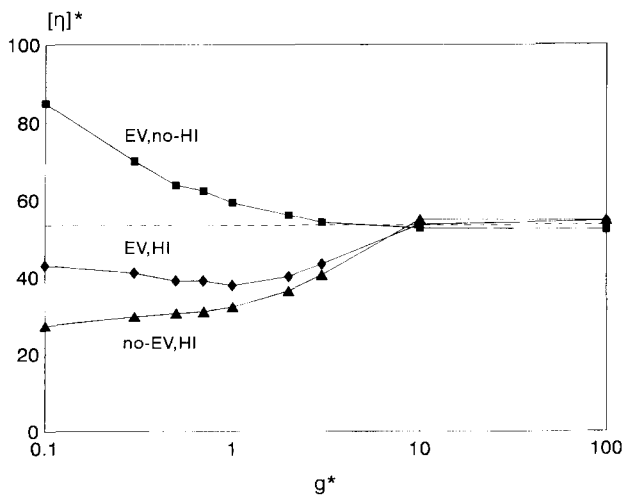

Figure 3 Intrinsic viscosity versus dimensionless shear rate for a 20-bead Gaussian chain. Three cases are shown: with EV and without HI (EV, no-HI); without EV and with HI (no-EV, HI); with EV and with HI (EV, HI)

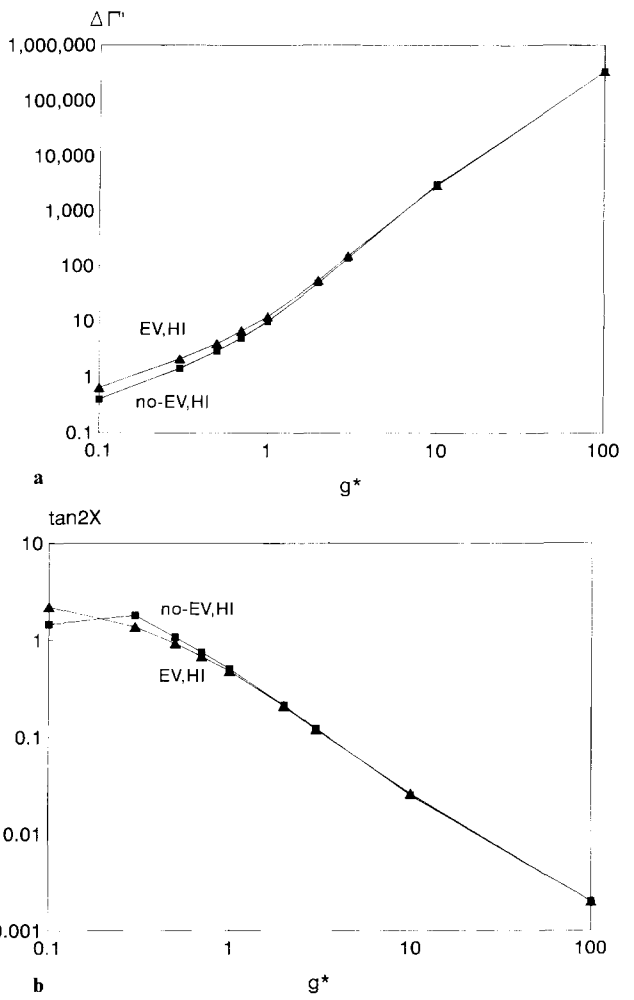

Figure 4 (a) Differential polarizability in reduced form, $\Delta\Gamma'$, *versus* dimensionless shear rate for a 20-bead Gaussian chain. Two cases are shown: without EV and with HI (no-EV, HI); with EV and with HI (EV, HI). (b) Extinction angle, $\tan 2\chi$, *versus* dimensionless shear rate for a 20-bead Gaussian chain. Two cases are shown: without EV and with HI (no-EV, HI); with EV and with HI (EV, HI)

earlier, and has disappeared at a shear rate $g^* = 10$, where the EV and no-EV curves coincide. The slope of $\Delta\Gamma'$ *versus* g^* in this region is equal to 2.0 ± 0.1. A result that is in accordance with theory[12] for this parameter and that also was observed in a previous work of ours[14], where excluded volume was not discussed. *Figure 4b* shows the other important parameter in flow birefringence studies, the extinction angle, presented in the form of $\tan 2\chi$. The value of this parameter falls with increasing shear rate since this corresponds to a more pronounced orientation of the polymer chains in the flow field. However, it shows the same qualitative behaviour as $\Delta\Gamma'$, with a significant EV-effect at low shear rates and disappearance of this effect at high shear. The slope of $\tan 2\chi$ *versus* g^* at high shear is the same as that for $\Delta\Gamma'$ (-2.0), in accordance with theory[12].

As mentioned in the Introduction, according to theory, the radius of gyration for a Gaussian chain in the no-EV, no-HI-case depends on the number of beads N to the power of 4 and on the shear rate g to the second power. The theoretical expression for $\langle S^2 \rangle$ can be put in the form: $\delta = (\langle S^2 \rangle - \langle S_0^2 \rangle)/\langle S_0^2 \rangle \propto N^4 g^2$. Thus, if we make a log–log plot of δ *versus* N we should get an exponent equal to 4. In *Figure 5a* is shown our simulation results for δ *versus* N for three different values of the shear rate, and with EV and HI included. We observe a shear rate dependence with a stronger influence of the number of beads in the chain (N) as the shear rate is increased. In *Figure 5b* we have plotted the value of the exponent over 3 decades of the shear rate. For the case without excluded volume and hydrodynamic interaction we obtain an exponent equal to 4.0 ± 0.2, in accordance with theory. When excluded volume and hydrodynamic interaction are taken into account, we obtain the same exponent for high values of the shear rate, corresponding to the disappearance of these two effects. However, for lower shear rates the exponent is found to be smaller, a result that indicates that for a real system, at shear rates low enough for excluded volume and hydrodynamic interaction to still have effect, the chain dimensions are less dependent on the molecular weight (i.e. number of beads) than in the more idealized no-EV, no-HI system.

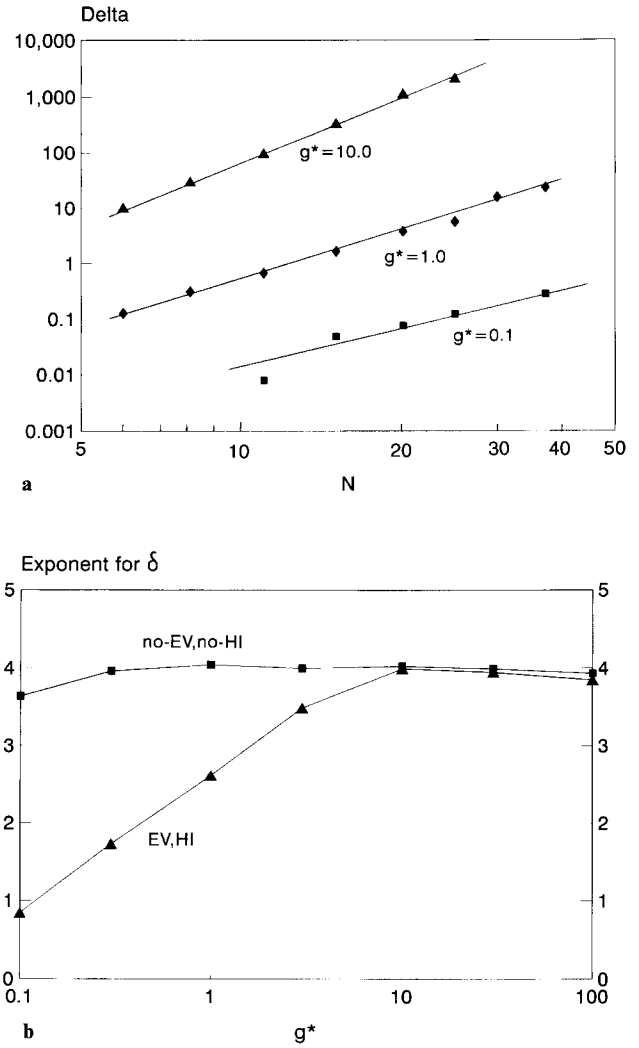

Figure 5 (a) Reduced radius of gyration, $\delta = (\langle S^2 \rangle - \langle S_0^2 \rangle)/\langle S_0^2 \rangle$, *versus* number of beads in the chain, N, for Gaussian chains at three different shear rates. The results shown are with HI included. (b) Value of exponent in the relation between δ (reduced radius of gyration) and N (number of beads in chain) *versus* dimensionless shear rate for Gaussian chains. Two cases are shown: without EV and without HI (no-EV, no-HI); with EV and with HI (EV, HI)

CONCLUSION

The use of the new type of 'soft-potential' proposed by Rey *et al.*[2,3] for describing the excluded volume effect in a flexible polymer chain has made possible the simulation study of the behaviour of the chain in steady shear, taking into account both excluded volume and hydrodynamic interaction at the same time. The validity of the approach has been checked comparing the results for the mean square radius of gyration and the mean square end–end distance at equilibrium with theoretical predictions, and the simulation results obtained for the parameters studied are generally in agreement with what one would expect from a qualitative discussion of the way excluded volume and hydrodynamic interaction influence the chain properties. There is however a discrepancy between the results obtained for the intrinsic viscosity at high shear (shear thickening) and what is found experimentally for flexible chains, indicating that further refinement of the interactions within the polymer chain is needed.

ACKNOWLEDGEMENTS

This work has been supported by a postdoctoral fellowship from the Norwegian Research Council for Science and the Humanities (NAVF) to K.D.K. Support to K.D.K. has also been provided by the Commission of the European Communities (grant number ERBCHBICT 940974). J.G.T. acknowledges support from grant PB93–1132 from Dirección General de Investigación Científica y Técnica (MEC) and PB93/17 from Comunidad Autónoma de la Region de Murcia.

REFERENCES

1 LeGuillou, J. C. and Zinn Justin, J. *Phys. Rev. Lett.* 1977, **39,** 95
2 Rey, A., Freire, J. J. and García de la Torre, J. *Macromolecules* 1991, **24,** 4666
3 Rey, A., Freire, J. J. and García de la Torre, J. *Polymer* 1992, **33,** 3477
4 García Bernal, J. M. and Tirado García, M. M. *Makromol. Chem.* 1991, **1992,** 935

5 Frisch, H. L., Pistoor, N., Sariban, A., Binder, K. and Fesjian, S. J. *J. Chem. Phys.* 1988, **89,** 5194
6 López Cascales, J. J., Navarro, S. and García de la Torre, J. *Macromolecules* 1992, **25,** 3574
7 Yamakawa, H. *J. Chem. Phys.* 170, **53,** 436
8 Ermak, D. L. and McCammon, J. A. *J. Chem. Phys.* 1978, **69,** 1352
9 Iniesta, A. and García de la Torre, J. *Polymer* 1991, **32,** 2015
10 López Cascales, J. J. and García de la Torre, J. *Polymer* 1991, **32,** 3359
11 Bird, R. B., Curtiss, C. F., Armstrong, R. C. and Hassager, O. 'Dynamics of Polymeric Liquids', Vol. 2, 'Kinetic Theory', Wiley, New York, 1977, p. 27
12 Yamakawa, H. 'Modern Theory of Polymer Solutions', Harper and Row, New York, 1971
13 Pistoor, N. and Binder, K. *Colloid Polym. Sci.* 1988, **266,** 132
14 Knudsen, K. D., Elgaaeter, A., López Cascales, J. J. and García de la Torre, J. *Macromolecules* 1993, **26,** 3851
15 Díaz, F. G., García de la Torre, J. and Freire, J. J. *Polymer* 1989, **30,** 259